

The study of thermal connecting of telecommunication optical fibers (SiO₂: GeO₂) and EDF (SiO₂: Al₂O₃, Er) fibers

M. RATUSZEK^{1*}, M.J. RATUSZEK¹, and J. HEJNA²

¹ Department of Telecommunication and Power Engineering, University of Technology and Life Sciences, 7 Kaliskiego St., 85-796 Bydgoszcz, Poland

² Institute of Materials Sciences and Applied Mechanics, Wrocław University of Technology, 25 Smoluchowskiego St., 50-370 Wrocław, Poland

Abstract. This paper presents the research on optimization of the splicing process in the electric arc of telecommunication optical fibers and erbium doped EDF fibers. The results of the calculations of diffusion coefficients GeO₂ in telecommunication optical fibers and diffusion coefficients Er and Al₂O₃ (together) in the fiber EDF are presented. Diffusion coefficients were determined for the fusion temperature in the electric arc $\approx 2000^\circ\text{C}$, on the basis of changes, along the splice, of spliced thermoluminescence intensity profiles of the fibers. On the basis of knowledge of diffusion coefficients simulation calculation of loss joints of MC SMF fiber (*Matched Cladding Single Mode Fiber* – SiO₂: GeO₂) and NZDS SMF (Non Zero Dispersion Shifted – Single Mode Fiber – SiO₂: GeO₂) with EDF (Erbium Doped Fiber – SiO₂: Al₂O₃, Er) was performed and presented as a function of diffusion time. Experimental studies of optimization of thermal connected MC SMF and NZDS SMF with EDF were presented and compared with theoretical results. This paper presents the results of microscopic observations of defects and diffusion, and X-ray microanalysis in the spliced areas of single-mode telecommunication optical fibers: MC SMF, NZDS-SMF and erbium doped active single mode optical fibers. Studies were performed with the use of the scanning electron microscope JSM5800LV and JSM6610A microscope equipped with EDS X-ray spectrometer. Results showing the influence of heating time on the diffusion of core dopants and the formation of deformations in the splice areas were presented.

Key words: single mode telecommunication optical fiber, erbium doped optical fiber, optical fiber splicing, splicing loss, dopant diffusion, loss measurement, reflectometry.

1. Introduction

It is necessary to connect various telecommunication fibers with each other. The most frequently used method is splicing in the electric arc. The thermal connection of fibers has been known for a long time [1–3], and commonly used due to quickly changing structures and types of fibers. It is still of a great interest, being the subject of theoretical and experimental investigations including optimization, characterization of such connections, and their influence on transmission parameters of the fiber route [4–8]. New kinds and types of single-mode telecommunication optical fibers are being constantly created and their connections are of a great practical significance. It does not concern only fibers which are strictly of a telecommunication character. Connecting photonic crystal fibers with each other and with telecommunication fibers [9, 10] or special ones - doped by rare earth elements (Er, Pr, Nd, Yb) [11–13], used most frequently in amplifiers and fiber lasers, has significant documentation and is of practical importance.

Splicing of fibers used for the construction of fiber amplifiers and fiber lasers with standardized telecommunication optical fibers is one of the most difficult process of thermal connecting of telecommunication optical fibers. This is mainly due to significant differences in the parameters of connected fibers, such as mode field diameters, profiles of the refrac-

tive index in cores and claddings – which corresponds to the dopants concentration and mode field distributions, differences in the types of dopants used as active ions or to increase/decrease refractive index in active and telecommunication fibers.

These optical fibers must be connected mostly because the conventional single-mode telecommunication optical fibers are commonly used as standard pigtailed, used for the endings of active fibers. In the fiber amplifiers and lasers, single-mode optical fibers are the most commonly used. They are usually made of the silica glass and their cores are doped with GeO₂ and/or Al₂O₃ and rare earth ions, the most often Er, Pr, Nd, Yb. These fibers, as already has been mentioned, should be connected to standard telecommunication fibers, which usually have larger mode field diameters and are not doped with rare earth elements, but with GeO₂ or GeO₂, and F.

The most frequent splice loss cause is the lack of a match of the spliced optical fibers mode field radii and then, with the assumption that fibers are connected centrally. The distribution of the main mode field LP_{01} can be approximated by the Gaussian distribution, the values of losses resulting from the lack of match of the mode fields can be achieved as [14, 15]:

$$A_\alpha = -10 \log \left[\left(2W_1W_2 / (W_1^2 + W_2^2) \right)^2 \right], \quad (1)$$

*e-mail: m.ratuszek@utp.edu.pl

where W_1, W_2 – mode fields radii of spliced fibers in the point of contact.

In order to avoid these losses, radii of mode fields W_1 and W_2 of spliced fibers must be matched. For this purpose a transit area must be formed in the spliced fibers, where mode radii matching will take place. In order to do so, work consuming methods of welding in pieces of fibers with successively increasing mode field radii can be applied between the spliced fibers [16]. However, it is better to create, by the method of core dopant controlled diffusion, an area of thermal diffusion TEC (*Thermally Expanded Core*), where mode fields matching takes place [5, 17, 18] – Fig. 1. Optimization of the process of fibers thermal connection with different parameters involves matching mode fields of fibers connected with the use of core dopant diffusion method [5, 17] and minimization of thermally diffused dopant transit area TEC loss [16–19] – Fig. 1.

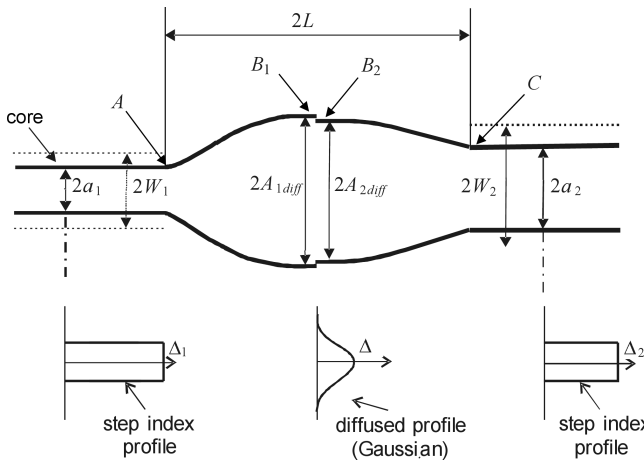


Fig. 1. Schematic illustration of the thermally diffused expanded core area of the spliced fibers with step refractive index profiles

Total splice loss of TEC area are a sum of losses resulting from the lack of match of mode field radii (after diffusion) and transmission losses T_f [7, 17, 19, 20]:

$$\Sigma = -10 \log \left[\left(\frac{2W_{diff1}W_{diff2}}{W_{diff1}^2 + W_{diff2}^2} \right)^2 \right] - 10 \log T_f, \quad (2)$$

where W_{diff1}, W_{diff2} – mode fields radii of connected fibers in the point of contact (after diffusion), in TEC, T_f – optical power transmission coefficient for TEC area resulting from its dimensions.

For the mode field radii equalizable, in the point of contact and their linear change in the transit area, the biggest splice loss for the area (the worst case) occurs with the minimum value of transmission coefficient T_f described as [7]:

$$T_f = T_A T_{B1} T_{B2} T_C, \quad (3)$$

where

$$T_A = \left[1 + \{0.5(\gamma_{max1} - 1)(\pi n_1 W_1^2 / \lambda L)\}^2 \right]^{-1}, \quad (4)$$

$$T_C = \left[1 + \{0.5(\gamma_{max2} - 1)(\pi n_2 W_2^2 / \lambda L)\}^2 \right]^{-1}, \quad (5)$$

$$T_{B1} = \left[1 + \{\gamma_{max1}(\gamma_{max1} - 1)(\pi n_1 W_1^2 / \lambda L)\}^2 \right]^{-1}, \quad (6)$$

$$T_{B2} = \left[1 + \{\gamma_{max2}(\gamma_{max2} - 1)(\pi n_2 W_2^2 / \lambda L)\}^2 \right]^{-1}, \quad (7)$$

where T_A, T_{B1}, T_{B2} and T_C – power transmission coefficients in points A, B₁, B₂ and C – Fig. 1, L – half of TEC area length – Fig. 1, $\gamma_{max} = A_{diff}/a$ is a ratio of the core radius after diffusion to the core radius before diffusion, n – core refractive index, W – mode field radius, λ – wavelength. In Eqs. (4)–(7) index 1 denotes parameters of input fiber (for example, of the type G.655 [21]), and index 2 output (e.g. of the type G.652 [22]).

For total loss calculations Σ (2) it is necessary to know the core dopant diffusion coefficients of spliced fibers and TEC area length – $2L$. Knowing diffusion coefficients, A_{diff} can be calculated [17]:

$$A_{diff} = \sqrt{a^2 + 4Dt}, \quad (8)$$

where D – diffusion coefficient, t – diffusion time.

Assuming the Gaussian distribution of the mode field LP_{01} we have [23]: $W = a/\sqrt{\ln V}$ where a and W are radii of the core and the mode field before diffusion. As the area of splice (TEC) remains of single mode character [17, 24, 25], normalized frequency $V = 2\pi aNA/\lambda$ remains unchanged after diffusion, thus, $W_{diff}/A_{diff} = 1/\sqrt{\ln V}$.

2. Fibers used for research

To studies on the optimization of spliced erbium-doped single-mode optical fibers and single mode telecommunication optical fibers the following fibers were used (Table 1):

- MC-SMF 1528 (Matched Cladding Single Mode Fiber) – Siecor (OVD – Outside Vapour Deposition) – step refractive index profile [26],
- NZDS SMF (Non Zero Dispersion Shifted – Single Mode Fiber) type: True Wave, refractive index profile type “crown” [27],
- EDF (Erbium Doped Fiber) – No. IIA (MCVD - Modified Chemical Vapour Deposition) – step refractive index profile [28],
- EDF (Erbium Doped Fiber) – No. IIB (MCVD) – step refractive index profile [28],
- EDF (Erbium Doped Fiber) – No. IIC (MCVD) – step refractive index profile [28].

Table 1
Parameters of fibers: EDF-IIA, EDF-IIB, EDF-IIC [28]

Parameters	EDF-IIA	EDF-IIB	EDF-IIC
Content of Er in the core	1000 ppm	1000 ppm	1000 ppm
Content of Al ₂ O ₃ in the core	10000 ppm	10000 ppm	10000 ppm
Cut-off wavelength λ_c	1250 nm	820 nm	1100 nm
Core diameter 2a	7.9 μm .	5.0 μm .	7.0 μm .

3. The calculations of the diffusion coefficients: GeO_2 in SiO_2 , Er and Al_2O_3 in SiO_2

The values of diffusion coefficients GeO_2 – i.e. core dopant in MC SMF and NZDS SMF were defined in [7, 8, 24] for the fusion temperature in the electric arc 1900–2000°C. In the core of optical fibers EDF there is Er and Al_2O_3 – which increases the refractive index of silica glass. It is not possible to use the method proposed in [8, 24] to determine separately the diffusion coefficients of Er in SiO_2 and Al_2O_3 in SiO_2 . The diffusion coefficient calculated with this method applies to both Er and Al_2O_3 .

To estimate the processes of diffusion of Er and Al_2O_3 the EDF-IIA, EDF-IIB and EDF-IIC optical fiber – Table 1 – and undoped silica glass rod with diameter of $\approx 130\mu\text{m}$ were used. The diffusion coefficients were calculated on the basis of changes along the splice, the intensity of thermoluminescence profiles of spliced fibers as shown for GeO_2 in Fig. 2 [8, 24]. During the examination of diffusion coefficients Er and Al_2O_3 in SiO_2 the splice temperature was 2000°C [25]. Splicing (diffusion) time was changed from 2 to 12 seconds. Linear dependence of thermoluminescence intensity on molar concentration of Er (initial concentration $C_{\text{Er}} = 0.1\%$ mol/mol) and Al_2O_3 (initial concentration $C_{\text{Al}_2\text{O}_3} = 1\%$ mol/mol in SiO_2 was assumed [28]). With the method suggested in [8, 24] the curves of changes of light intensity for different splicing times as a function of distance from the front of the splice was obtained.

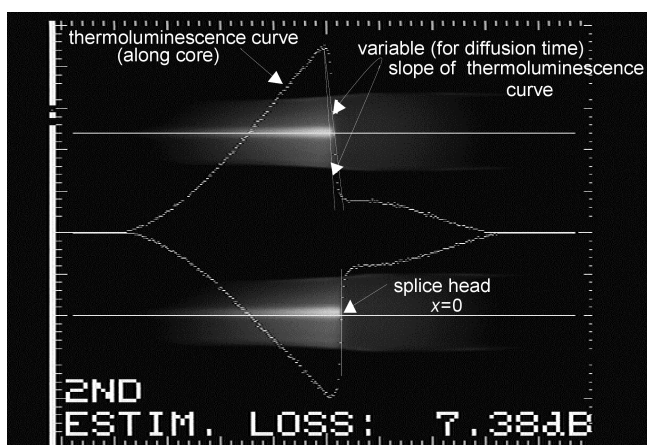


Fig. 2. Exemplary thermo-luminescence intensity profile for $t = 6$ s

The molar concentration of Er in SiO_2 and Al_2O_3 in SiO_2 , in the initial dopant concentrations in core EDF fibers, were assigned. They had the following values: $N_{0\text{Er}} = 2.19 \cdot 10^{25} \text{ m}^{-3}$ and $N_{0\text{Al}_2\text{O}_3} = 2.19 \cdot 10^{26} \text{ m}^{-3}$. Knowing N_0 (Er and Al_2O_3), x , t and defining $N(x, t)$, on the basis of thermoluminescence intensity changes, diffusion coefficients D of Er and Al_2O_3 in SiO_2 at $\approx 2000^\circ\text{C}$ were calculated. Er and Al_2O_3 diffusion coefficients in the range of the linear decrease of thermoluminescence curve for the distance $x = 10 \mu\text{m}$ and $x = 15 \mu\text{m}$ from the front of a joint were calculated.

Values of the diffusion coefficients changing in the range $D = 10^{-13} \div 5 \cdot 10^{-13} \text{ m}^2/\text{s}$ were obtained. Results of studies of diffusion coefficients GeO_2 in SiO_2 at $\approx 2000^\circ\text{C}$

presented in [8, 24] gave values within the range: $D = 10^{-13} \div 10^{-12} \text{ m}^2/\text{s}$. So, it is the range within the interval of diffusion coefficients of Er and Al_2O_3 in SiO_2 at $\approx 2000^\circ\text{C}$. It allows to assume the same range of values of diffusion coefficients ($D = 10^{-13} \div 10^{-12} \text{ m}^2/\text{s}$) Er and Al_2O_3 in SiO_2 and GeO_2 in SiO_2 . This greatly simplifies the simulation and optimization of losses (splicing time) in thermal connections of fibers doped with Er and Al_2O_3 and GeO_2 . The literature does not provide data about the values of diffusion coefficients Er and Al_2O_3 and GeO_2 in SiO_2 in the temperature $\approx 2000^\circ\text{C}$. Extrapolation [29] of the temperature dependence of diffusion coefficients D GeO_2 in SiO_2 , in temperature range 1200–1600°C, to the temperature 1900–2000°C, gave values within the range: $D = 10^{-14} \div 10^{-12} \text{ m}^2/\text{s}$.

4. Losses in the TEC area of thermally connected fibers – theoretical analysis

Total losses of optical power in TEC area are the sum of losses resulting from the mismatch of mode field radiuses and the transit area size TEC [5–7]. Analysis of the two variables allows to match the optimal time of thermal connecting. In Figs. 3–6 hypothetical dependence of total losses of TEC areas on diffusion time (2): $\sum(t) = A_\alpha(t) - 10 \log T_f(t)$ was presented for diffusion coefficients from the range $D = 10^{-13} \div 5 \cdot 10^{-13} \text{ m}^2/\text{s}$ and TEC area length: $2L = 700 \mu\text{m}$ – which corresponds to the length of the heating area for the arc of the fusion splicers [8, 24].

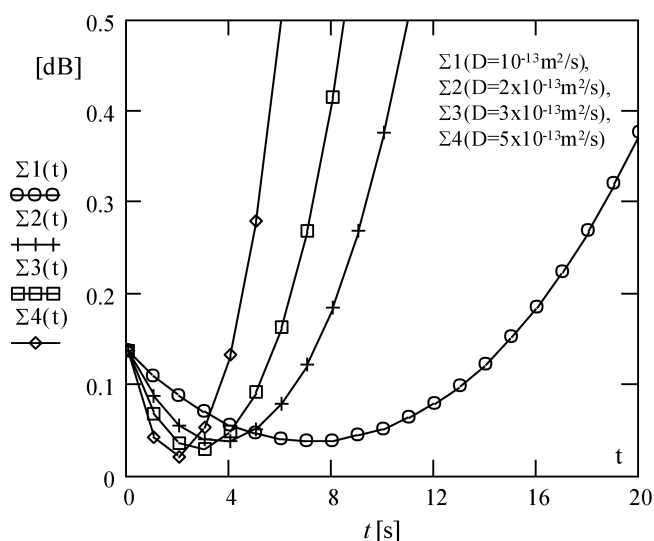


Fig. 3. The dependence of the total loss Σ (dB) of TEC area on diffusion time (t sec.) for the connections of EDF-IIB and MC SMF fibers and diffusion coefficients: $\Sigma 1$ ($D = 10^{-13} \text{ m}^2/\text{s}$), $\Sigma 2$ ($D = 2 \times 10^{-13} \text{ m}^2/\text{s}$), $\Sigma 3$ ($D = 3 \times 10^{-13} \text{ m}^2/\text{s}$), $\Sigma 4$ ($D = 5 \times 10^{-13} \text{ m}^2/\text{s}$); $L = 350 \mu\text{m}$, $\lambda = 1.31 \mu\text{m}$

In Fig. 3 to 6 two types of diffusion processes were presented. In the first process (Figs. 3–4) equality of diffusion coefficients Er and Al_2O_3 in SiO_2 and GeO_2 in SiO_2 was assumed, i.e. the equality of these coefficients in the fibers: EDF-IIA, B and MC SMF and NZDS SMF. Because generally at higher dopant concentrations increasing of their

diffusion coefficients is observed [30] in the second case (Figs. 5–6) higher values of diffusion coefficients in optical fibers MC SMF (content of GeO₂ in the core of approximately 35000 ppm) and NZDS SMF (GeO₂ in the core content of about 50000 ppm) than in the optical fibers EDF-IIA, B, C were assumed (Table 1).

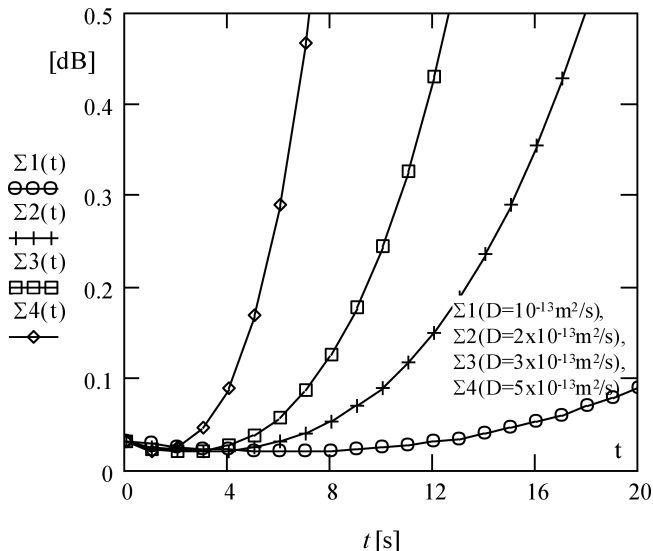


Fig. 4. The dependence of the total loss Σ (dB) of TEC area on diffusion time (t sec.) for the connections of EDF-IIA and NZDS SMF fibers and diffusion coefficients: $\Sigma 1$ ($D = 10^{-13} \text{ m}^2/\text{s}$), $\Sigma 2$ ($D = 2 \times 10^{-13} \text{ m}^2/\text{s}$), $\Sigma 3$ ($D = 3 \times 10^{-13} \text{ m}^2/\text{s}$), $\Sigma 4$ ($D = 5 \times 10^{-13} \text{ m}^2/\text{s}$); $L = 350 \mu\text{m}$, $\lambda = 1.31 \mu\text{m}$

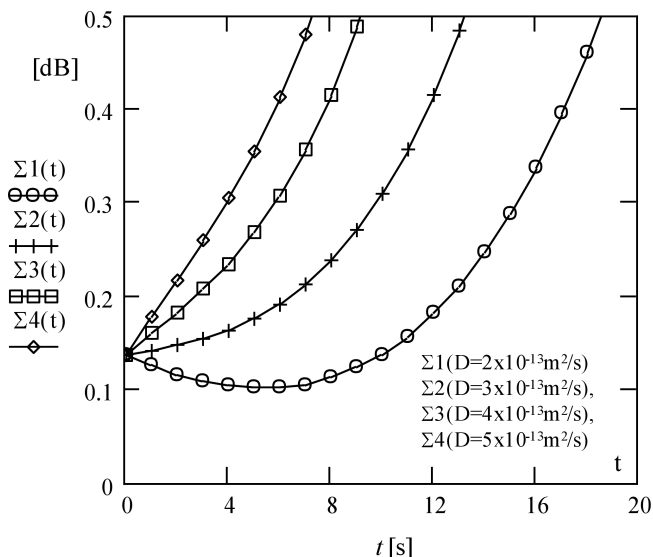


Fig. 5. The dependence of the total loss Σ (dB) of TEC area on diffusion time (t sec.) for connections of EDF-IIB and MC SMF fibers – constant diffusion coefficient E_r and Al_2O_3 in EDF: $D = 10^{-13} \text{ m}^2/\text{s}$ and diffusion coefficients GeO_2 in MC SMF: $\Sigma 1$ ($D = 2 \times 10^{-13} \text{ m}^2/\text{s}$), $\Sigma 2$ ($D = 3 \times 10^{-13} \text{ m}^2/\text{s}$), $\Sigma 3$ ($D = 4 \times 10^{-13} \text{ m}^2/\text{s}$), $\Sigma 4$ ($D = 5 \times 10^{-13} \text{ m}^2/\text{s}$); $L = 350 \mu\text{m}$, $\lambda = 1.31 \mu\text{m}$

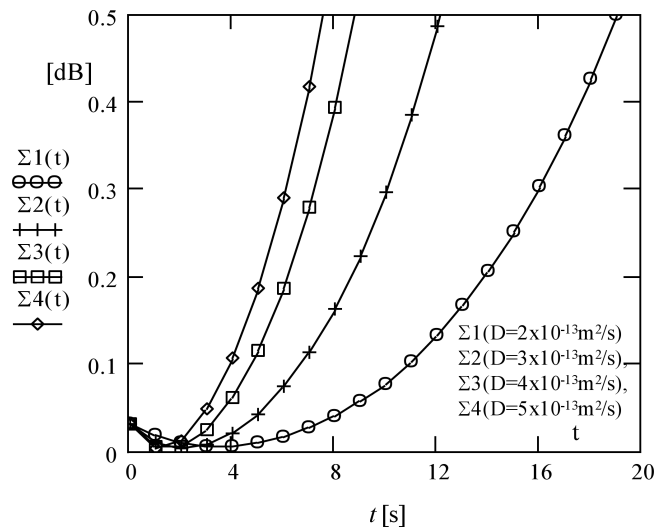


Fig. 6. The dependence of the total loss Σ (dB) of TEC area on diffusion time (t sec.) for the connections of EDF-IIA and NZDS SMF fibers – constant diffusion coefficient E_r and Al_2O_3 in EDF: $D = 10^{-13} \text{ m}^2/\text{s}$ and diffusion coefficients GeO_2 in MC SMF: $\Sigma 1$ ($D = 2 \times 10^{-13} \text{ m}^2/\text{s}$), $\Sigma 2$ ($D = 3 \times 10^{-13} \text{ m}^2/\text{s}$), $\Sigma 3$ ($D = 4 \times 10^{-13} \text{ m}^2/\text{s}$), $\Sigma 4$ ($D = 5 \times 10^{-13} \text{ m}^2/\text{s}$), $L = 350 \mu\text{m}$, $\lambda = 1.31 \mu\text{m}$

4.1. Conclusions from the simulation of optimization of splicing fibers The assumption of the same values of dopant core diffusion coefficients in connected fibers showed that optimization (increasing of splicing time over the standard 2 seconds) requires connection of EDF-IIB and the MC SMF fibers – Fig. 3. Simulation showed that in this case we should try to modify the splicing time from 2 to 8 seconds. Connecting times from 2 to 8 seconds for connections of EDF-IIA and NZDS SMF – Fig. 4 can be changed as well. Assuming a constant value of the core dopant diffusion coefficients in the EDF-IIA,B (different diameters of the cores at the same levels of doping E_r and Al_2O_3 in SiO_2) and higher values of dopant diffusion coefficients GeO_2 in fibers MC SMF and NZDS SMF the combination of EDF-IIB and MC SMF – Fig. 5 and EDF-IIA and NZDS SMF – Fig. 6 requires optimization. Here, splicing time can be changed from 2 to 6 seconds. In other cases, the splicing does not require optimization and connecting procedures may be used, as you would, in standard, single-mode telecommunication fibers with slightly different parameters [24].

5. Experimental studies of optimization of thermal connections of single-mode EDF fibers with NZDS SMF and MC SMF fibers

During the experimental studies of optimization, fibers were connected together in the following combinations: EDF-IIB and MC SMF, EDF-IIA and NZDS SMF. The verification of splices, meant for measuring, was performed by analyzing the pictures of thermoluminescence hot splices. Pictures of thermoluminescence were obtained using Ericsson FSU 925 RTC fusion splicer. Time of the main splicing stage was being changed from 2 to 10 seconds. It should be underlined that the

standard fusion current (keeping the temperature $\approx 2000^\circ\text{C}$) and the splicing time for fibers MC SMF are $I = 16 \div 17$ mA and $t = 2$ seconds [24, 25].

Splices loss measurements were conducted with a use of reflectometry method [31]. Loss measurements were conducted with reflectometer MW9070B Anritsu, which has four measurement wavelengths: $\lambda = 1310, 1450, 1550,$ and 1625 nm [31]. Nevertheless, measurements only for $\lambda = 1310$ nm could be done effectively, for the other wavelengths EDF have very high attenuation (which is a characteristic and positive for fibers designed for amplifying medium in the third optical window) and dynamics of reflectometer is too low (30 dB) to distinguish signal from noise behind the splice.

The length of EDF fibers used in the tests was 10 m. The transmission method of measurement was used for $\lambda = 1550$ nm, losses of a 10-meter segments. Losses amounted to: EDF-IIA (10 m): 22.88 dB ($\lambda = 1550$ nm); EDF-IIB (10 m): 28.73 dB ($\lambda = 1550$ nm); EDF-IIC (10 m): 24.16 dB ($\lambda = 1550$ nm). And for $\lambda = 1310$ nm losses were as follows: EDF-IIA (10 m): 0.47 dB ($\lambda = 1310$ nm); EDF-IIB (10 m): 1.34 dB ($\lambda = 1310$ nm); EDF-IIC (10 m): 0.54 dB ($\lambda = 1310$ nm). These measurements were important because the short lengths of EDF gave on the reflectometric figures common with the splice picture of loss and loss of fiber had to be separated from the splice.

Results of simulations $\sum(t) = A_\alpha(t) - 10 \log T_f(t)$ and reflectometric measurements $A_s(t)$ of splice losses for fibers EDF-IIB-MC SMF and EDF-IIA-NZDS SMF, for five connection times and different diffusion coefficients – hence the min-max in the Tables 2–3.

Table 2

Summary of theoretical: $\sum = A_\alpha - 10 \log T_f$ – Fig. 3 and Fig. 5 and experimental A_s results of splice losses: EDF-IIB and MC SMF fibers

Splicing time [s]	Σ [dB] – Fig. 3 [min÷max]	Σ [dB] – Fig. 5 [min÷max]	A_s [dB] $\lambda = 1310$ nm
2	0.02÷0.09	0.12÷0.23	0.22
3	0.025÷0.07	0.11÷0.25	0.23
5	0.05÷0.34	0.10÷0.38	0.33
7	0.04÷1.0	0.11÷0.46	0.50
10	0.05÷2.8	0.14÷1.0	0.52

Table 3

Summary of theoretical: $\sum = A_\alpha - 10 \log T_f$ – Fig. 4 and Fig. 6 and experimental A_s results of splice losses: EDF-IIA and NZDS SMF fibers

Splicing time [s]	Σ [dB] – Fig. 3 [min÷max]	Σ [dB] – Fig. 5 [min÷max]	A_s [dB] $\lambda = 1310$ nm
2	0.02÷0.025	0.01÷0.012	0.23
3	0.02÷0.05	0.01÷0.15	0.29
5	0.02÷0.15	0.02÷0.25	0.33
7	0.02÷0.5	0.04÷0.5	0.41
10	0.025÷2.0	0.1÷1.2	0.49

6. Studies of splices with use of scanning electron microscopy and X-ray microanalysis

Microscopic observations and microanalysis of splices can directly provide information on the size and composition of

TEC transit area, as well as demonstrate the continuity of structures within the splice [32–34] and the lack of structure areas separate from the amorphous SiO_2 .

Observation of splices and X-ray microanalysis were conducted with the scanning microscope JEOL JSM5800LV. This is a standard SEM with a thermionic electron gun. The microscope was equipped in a semiconductor detector for backscattered electrons and an energy dispersive spectrometer (Oxford ISIS 300) for X-rays. The microscope was used in a standard high vacuum mode ($p \approx 10^{-2}$ Pa) and in a low vacuum mode ($p = 45$ Pa). The low vacuum mode enables to observe insulators without a conductive coating. As mentioned earlier, the low vacuum mode was used to control the grinding process. Before final examinations specimens were coated with carbon layers and observed in the high vacuum mode.

Description of sample preparation, microscopic examination and X-ray microanalysis of splices composition was presented in [34].

6.1. Microscopic observations of splices. Examples of microscopic pictures of splices of tested fibers were presented in Figs. 7–11. The identification of connected fiber types, the time of splicing, and zoom (symbol x) were included in the captions.

Microscopic observations showed continuity and lack of structural changes in examined splices. The observations also allowed to eliminate from the loss measurements splices where non-concentric splicing or core deformation due to long heating time occurred. This should be taken into account, that the study confirmed the high circularity of cladding and centric location of cores. In the case of long splicing time (Fig. 11), loss of sharpness, and rounding in the splice area may be evidence for the diffusion of dopant core. Additionally, clearly visible refractive index profile can be observed on the microscopic view. It is very useful for analysis of splices connecting unknown optical fibers.

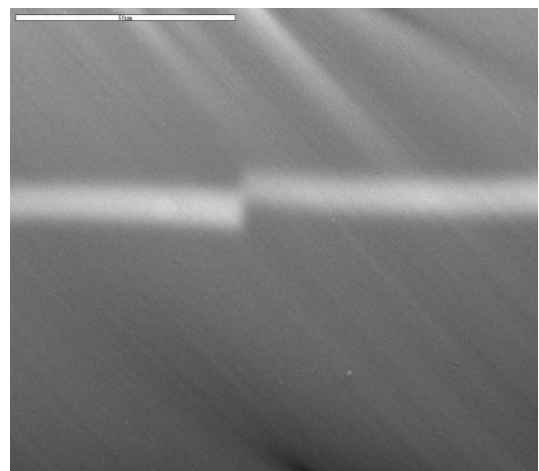


Fig. 7. Left: MC SMF – right: EDF-IIA; splicing time 10 sec. $\times 1000$. Comparable core diameters in the MC SMF ($8.3 \mu\text{m}$) and in EDF-IIA ($7.9 \mu\text{m}$). Splice done properly, but as a result of long connecting time core deformation on the forehead of joints occurred. Splice not taken into account in the measurement

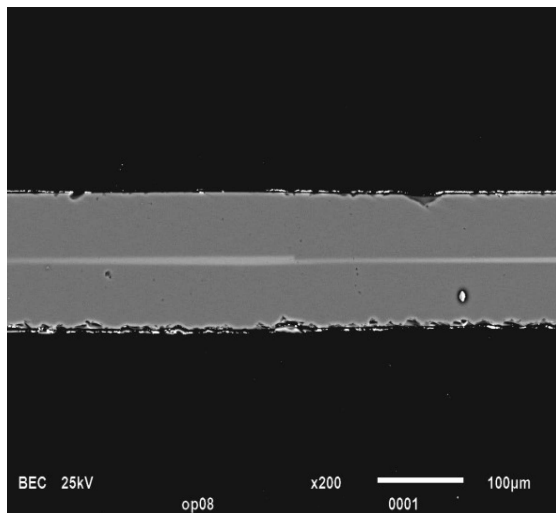


Fig. 8. Left: MC SMF – right: EDF-IIB; splicing time 3 sec. x200. Clearly visible differences in the core diameters in the MC SMF (8.3 μm) and in EDF-IIB (5 μm). Splice done incorrectly: clear eccentric connecting of cores. Splice not taken into account in the measurement

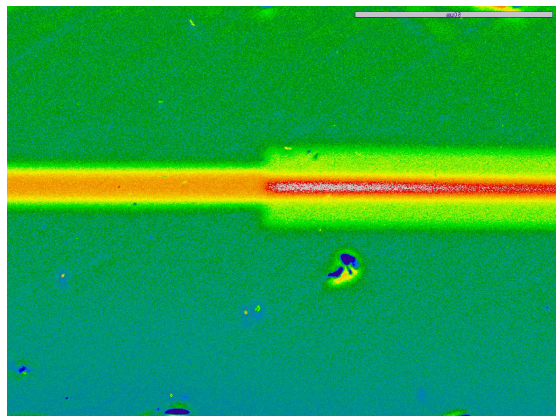


Fig. 9. Left: EDF-IIA – right: NZDS SMF; splicing time 5 sec. x1000. Clearly visible refractive index profile, type: crown, in NZDS SMF. Splice done correctly

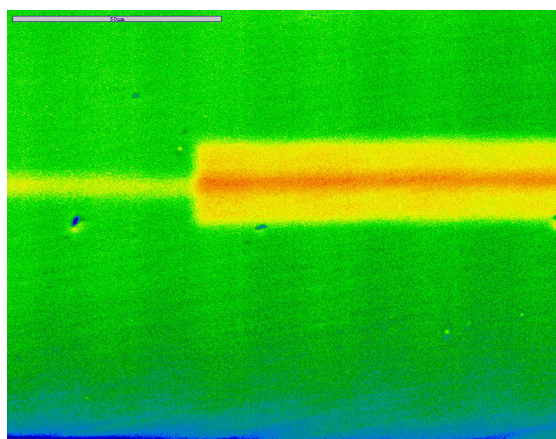


Fig. 10. Left: EDF-IIB – right: NZDS SMF; splicing time 5 sec. x1000. Clearly visible refractive index profile, crown type, in NZDS SMF. Clearly visible differences in the cores diameters in the EDF-IIB (5 μm) and EDF-IIA (7.9 μm) – Fig. 9. Splice done correctly

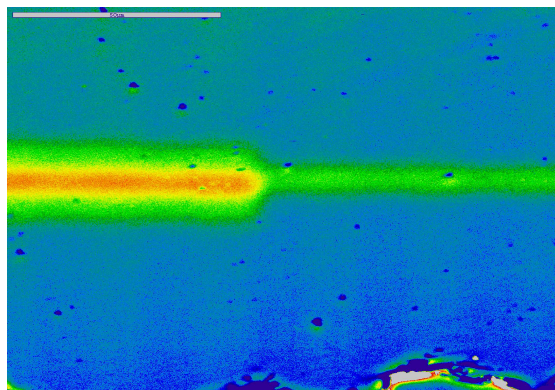


Fig. 11. Left: NZDS SMF – right: EDF-IIB; splicing time – 12 sec. x1000. Clearly visible refractive index profile, crown type, in NZDS SMF. In case of long splicing time (12 sec.) loss of sharpness in the splice area may be evidence of diffusion of dopant core. Splice done correctly

6.2. X-ray microanalysis of fiber splices Microanalysis was performed for three samples: 1) splice EDF-IIB and NZDS SMF- splicing time 5 sec., 2) splice EDF-IIB and NZDS SMF – splicing time 10 sec., 3) splice EDF-IIA and silica rod – splicing time 10 sec. The points of analysis, on the example of the connection of EDF-IIB and NZDS SMF, are presented in Fig. 12. The analysis is qualitative, since the sensitivity of the device was 1 at% (10000ppm). Sample microanalysis are presented below in Figs. 13–14.

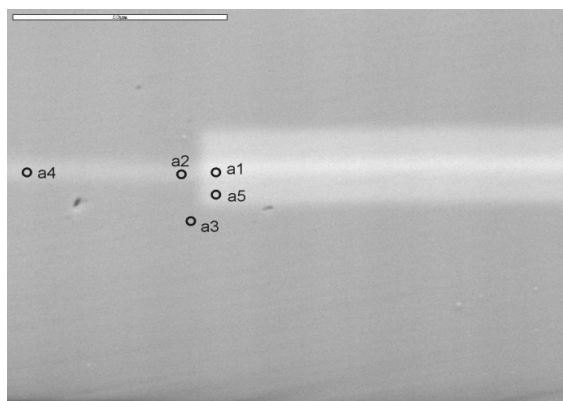


Fig. 12. Points of microanalysis – on the example of joint EDF-IIB (left) and NZDS SMF (right)

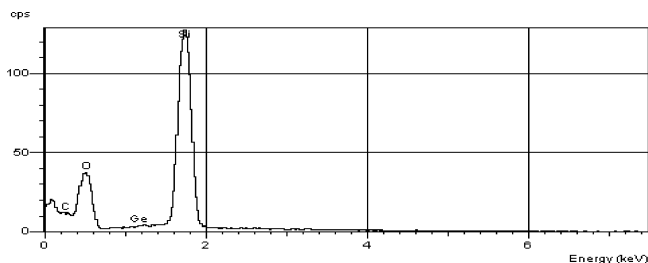


Fig. 13. Microanalysis at the point a3 – joint EDF-IIB and the NZDS SMF – splicing time 5 sec.

Presence of traces of Ge at the point a3 (Fig. 12) can be confirmed (Figs. 13–14) on the basis of X-ray microanalysis only qualitatively GeO_2 diffusion in the process of thermal

connecting. No indication of the presence of Er in the tested points. This is the result of the sensitivity of the method, which is 1 at%, and erbium in the fibers is about 0.1 at%. The presence of Al was not observed. Al amounts in the fibers to 1 at%, but the possible peak of Al neighbors on powerful Si peak and, hence, may not be visible.

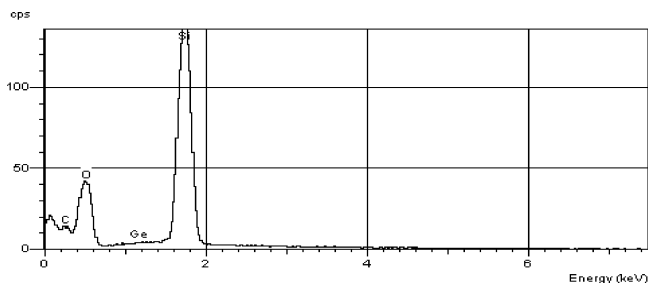


Fig. 14. Microanalysis at the point a3 – joint EDF-IIB and the NZDS SMF – splicing time 10 sec.

7. Conclusions

Formation of the transit area of sufficient length L , with optimally matched mode fields radii after diffusion (W_{diff1} , E_{diff2}) and numerical apertures NA (refractive index in the cores), within the TEC of connected fibers, is related with the processes of equalization of dopant concentration (usually GeO_2) in this area. In the cores of examined EDF fibers, there is Er and Al_2O_3 . Al_2O_3 increases the refractive index of silica glass, and Er makes SiO_2 the active environment with optical waves. It is impossible to determine separately the values of diffusion coefficients i.e. Er in SiO_2 and Al_2O_3 in SiO_2 with the method suggested in the paper. Diffusion coefficient calculated in this way applies together to Er and Al_2O_3 .

The results of experiments – Tables 2–3 indicate that EDF fibers doped with Al_2O_3 hardly can be subject to optimization of the connecting with fibers doped with GeO_2 . Moreover, splice losses are greater than those resulting only from the mismatch between the mode field diameters of connected fibers - simulation results for time $t = 0$ sec. – Figs. 3–6. Comparison of simulation results with the results of experimental tests indicates two possible causes of divergence. Firstly, mainly erbium diffuses into cladding, and Al_2O_3 remains in the core without increasing mode field diameter of the EDF fiber. At this time, the diffusion of core dopant (GeO_2) in telecommunication fibers occurs. As a consequence, an increase in the differences in the mode field diameters of connected fibers occurs. That would explain the higher loss of optimized splices than the one resulting only from the mismatch of mode field diameters of the same fibers. Thus, in this case, it is not possible to match mode field diameters in the process of diffusion, because there is here the reverse process. Secondly, and less probably, according to the authors, the diffusion Al_2O_3 is greater to SiO_2+GeO_2 (along the EDF core to the telecommunication fiber core) than to the EDF clad made of pure SiO_2 . This reduces the mode field diameter of EDF fiber on the forehead of the joint. However, diffusion of GeO_2 increases the mode field diameter of telecommunication fiber.

As a consequence, ditto, an increase in the differences of the mode field diameters of connected optical fibers occurs.

Observations with the use of scanning electron microscopy showed the continuity and lack of structural changes in the examined splices. Observations also allowed to eliminate from the loss measurements the splices where non-concentric splicing or core deformation due to long heating time occurred. Nevertheless, the study confirmed the high circularity of cladding and centric location of the cores relative to the claddings. On the basis of X-ray microanalysis only qualitatively GeO_2 diffusion in the process of thermal connecting, can be confirmed – Figs. 13–14 – presence of traces of Ge at the point a3. No indication of the presence of Er in the tested points. This is the result of the sensitivity of the method, which is 1 at%, and erbium in the fibers is about 0.1 at%.

Acknowledgements. This work was supported in part by the Polish Ministry of Science and Higher Education under the Grant NN517 397634.

REFERENCES

- [1] J.-I. Sakai and T. Kimura, “Splicing and bending losses of single-mode optical fibers”, *App. Opt.* 17, 3653–3659 (1978).
- [2] J.T. Krause, W.A. Reed, and K.L. Walker, “Splice loss of single-mode fiber as related to fusion time, temperature, and index profile alteration”, *J. Lightwave Technol.* LT-4, 837–840 (1986).
- [3] K. Shigihara, K. Shiraishi, and K. Kawakami, “Mode field transforming fiber between dissimilar waveguides”, *J. Appl. Phys.* 60, 4293–4298 (1986).
- [4] A.D. Yabloon, *Optical Fiber Fusion Splicing*, Springer Verlag, Berlin, 2005.
- [5] M. Ratuszek, J. Majewski, Z. Zakrzewski, and M.J. Ratuszek, “Process optimization of the arc fusion splicing different types of single mode telecommunication fibers”, *Opto-Electron. Rev.* 8, 161–170 (2000).
- [6] M. Ratuszek, “Analysis of reflectometric measurements losses of spliced single mode telecommunication fibers with significantly different parameters”, *Optica Applicata XXXV*, 347–363 (2005).
- [7] M. Ratuszek, “Analysis of loss of single mode telecommunication fiber thermally diffused core area”, *Optica Applicata XXXVII*, 279–294 (2007).
- [8] M. Ratuszek, Z. Zakrzewski, and J. Majewski, “Characteristics of thermally diffused transit areas of single-mode telecommunication fibers”, *J. Lightwave Technol.* 27, 3050–3056 (2009).
- [9] J.T. Lizier and G.E. Town, “Splice losses in holey optical fibers”, *IEEE Photon. Technol. Lett.* 13, 794–796 (2001).
- [10] F. Couny, F. Benabid, and P.S. Light, “Reduction of Fresnel back-reflection at splice interface between hollow core PCF and single-mode fiber”, *IEEE Photon. Technol. Lett.* 19, 1020–1022 (2007).
- [11] W. Zheng, O. Hulten, and R. Rylander, “Erbium-doped fiber splicing and splice loss estimation”, *J. Lightwave Technol.* 12, 430–435 (1994).
- [12] T. Veng and B. Palsdottir, “Investigation and optimization of fusion splicing abilities between erbium-doped optical fibres and standard singlemode fibres”, *Electron. Lett.* 41, 10–11 (2005).

- [13] A. Zając, D. Dorosz, M. Kochanowicz, M. Skórczakowski, and J. Świdorski, "Fiber lasers – conditioning constructional and technological", *Bull. Pol. Ac.: Tech.* 58, 491–502 (2010).
- [14] A.W. Snyder and J.D. Love, *Optical Waveguide Theory*, Chapman and Hall, London, 1983.
- [15] A. Majewski, *Theory and Design of Waveguides*, WNT, Warszawa, 1991, (in Polish).
- [16] N. Tomoyuki, O.Taichi, K. Kengo, N. Masashi, and T. Kotaro, "Fiber for next-generation extra-large-capacity DWDM transmission", *Hitachi Cable Rev.* 20, 3–6 (2001).
- [17] K. Shiraishi, Y. Aizawa, and S. Kawakami, "Beam expanding fiber using thermal diffusion of the dopant", *J. Lightwave Technol.* 8, 1151–1161 (1990).
- [18] W. Zheng, "Real time control of arc fusion for optical fiber splicing", *J. Lightwave Technol.* 11, 548–553 (1993).
- [19] T. Haibara, T. Nakashima, M. Matsnmoto, and H. Hanafusa, "Connection loss reduction by thermally-diffused expanded core fiber", *IEEE Photon. Technol. Lett.* 3, 348–350 (1991).
- [20] M. Ratuszek, "Analysis of loss of single mode telecommunication fiber thermally diffused core areas", *Proc. SPIE* 6608, 660817-16 (2007).
- [21] Recommendation ITU-T G.655, *Transmission Media Characteristics: Characteristics of a Non-Zero Dispersion Shifted Single Mode Optical Fibre Cable*, 2003.
- [22] Recommendation ITU-T G.652, *Transmission Media Characteristics: Characteristics of a Single-Mode Optical Fibre Cable*, 2003.
- [23] D. Marcuse, "Microdeformation losses of single mode fibers", *Appl. Opt.* 23, 1082–1091 (1984).
- [24] M. Ratuszek, "Thermal connections of one-mode telecommunication waveguides", *Habilitation Thesis*, Publishin House of the University of Technology and Life Sciences, Bydgoszcz, 2008, (in Polish).
- [25] W. Zheng, "The real time control technique for erbium doped fiber splicing", *Ericsson Rev.* 1, 1–24 (1993).
- [26] Fiber Focus – Corning, *Commercial Brochure with Introduction to Optical Fiber Standards*, 1998.
- [27] TruWave® Singlemode Optical Fiber – Lucent Technologies, *Brochure*, 1998.
- [28] J. Wójcik, "Methodology and fabrication parameters of EDF", *Unwritten Information*, UMCS, Lublin, 1998.
- [29] H. Yamada and H. Hanafusa, "Mode shape converter produced by the thermal diffusion of different dopants", *IEEE Photon. Technol. Lett.* 6, 531–533 (1994).
- [30] W. Jost, *Diffusion in Solids, Liquids, Gases*, Academic Press, New York, 1960.
- [31] M. Ratuszek, Z. Zakrzewski, and J. Majewski, "Reflectometric measurements of thermally expanded core area", *Bull. Pol. Ac.: Tech.* 58, 513–519 (2010).
- [32] J. Hejna, M. Ratuszek, Z. Zakrzewski, J. Majewski, and J. Wójcik, "Microscopic observations of defects and diffusion in one-mode joints of telecommunication waveguides doped with erbium", *Telecom. Review* 8–9, 826–835 (2010), (in Polish).
- [33] T-A. Wei and B.T. Devlin, "Analysis of optical fiber splices by the nondestructive x-ray imaging technique", *Proc. SPIE* 1791, 25–30 (1993).
- [34] J. Hejna, M. Ratuszek, J. Majewski, and Z. Zakrzewski, "Scanning electron microscope examination of telecommunication single mode fiber splices", *Optica Applicata XXXIII*, 583–589 (2003).